



Research

# Influence of the process parameters on the grinding result in continuous generating grinding of cutting tools

Berend Denkena<sup>1</sup> · Benjamin Bergmann<sup>1</sup> · Philipp Wolters<sup>1</sup> · Niklas Gärtner<sup>1</sup>

Received: 13 July 2023 / Accepted: 18 September 2023

Published online: 25 September 2023

© The Author(s) 2023 [OPEN](#)

## Abstract

Continuous generating grinding processes have largely replaced discontinuous profile grinding processes in gear manufacturing due to their higher productivity. On order to transfer the advantage of the productivity benefits of this process to tool grinding, the continuous generating grinding was adapted to the manufacture of cutting tools. However, this novel approach of using continuous generating grinding processes for tool grinding has not been widely investigated. Therefore, the aim of this study is to investigate the influence of cutting speed, feed and radial depth of cut on the process result and thus to generate initial knowledge for the process design. Subsequently, the influence of these parameters on the grinding worm wear as well as on the cutting edge quality and surface properties of the ground milling tools are investigated. The results show that an increase of the radial depth of cut leads to a reduction of the process time by the factor of four without significantly influencing the wear of the grinding worm tooth. Furthermore, an increase of the cutting speed only leads to an increase in the initial wear of the grinding worm after the dressing process. For this reason, the cutting speed offers the potential to further increase the productivity of the process. The microgeometry of the cutting edge of the ground milling tool is mainly affected by the feed and the macro geometry by the feed and radial depth of cut.

## Article highlights

- Determination of recommendations for the process design of continuous generating grinding for the production of cutting tools.
- Evaluation of the influence of the process parameters cutting speed, feed and depth of cut on the wear behaviour of grinding worms.
- Knowledge of the process parameters cutting speed, feed and radial depth of cut on milling tools.

**Keywords** Continuous generating grinding · Tool grinding · Cutting tools · Milling tools · Flute grinding

## List of symbols

$a_e$	Radial depth of cut	DTRQ	Disturbance torque
$c_p^*$	Normalized tip clearance	f	Feed
d	Outer diameter	h	Number of strokes
$d_k$	Core diameter	$m_n$	Normal module
		$q_d$	Dressing speed ratio

✉ Niklas Gärtner, gaertner@ifw.uni-hannover.de | <sup>1</sup>Institute of Production Engineering and Machine Tools (IFW), Leibniz University Hannover, An der Universität 2, 30823 Garbsen, Germany.



$Q_w$	Material removal rate
$R_a$	Average arithmetic roughness
$R_z$	Roughness depth
$v_c$	Cutting speed
$v_{cd}$	Cutting speed during dressing
$x^*$	Normalized addendum modification
$\alpha$	Clearance angle
$\alpha_{fp,l}$	Tooth root angle
$\gamma$	Rake angle

## 1 Introduction

The availability of high-quality cutting tools is a fundamental requirement for enabling the implementation of modern manufacturing processes. For the production of a lot of technical products, high precision tools like end mills, drilling tools or saw blades are essential. In most cases, discontinuous grinding processes are used to produce these cutting tools. In many of these processes different grinding wheels are used in succession to grind the different features of the cutting tools like e.g. the flutes, rake or flank faces. This discontinuous grinding processes are therefore accompanied by auxiliary process times resulting from the need to change the grinding wheel and the related kinematics which limit their productivity and can even influence the precision of the tool grinding process [1]. The increasing demand for cutting tools on the world market, however, creates the necessity to increase the productivity of tool grinding processes while maintaining their ability to produce cutting tools of high quality. It is therefore necessary to enhance the performance of already existing tool grinding processes or to develop entirely new processes for the manufacturing of cutting tools. With regard to conventional discontinuous tool grinding processes research approaches often focus on an optimisation of the grinding wheel properties and the process parameters. Examples for these are investigations concerned with an optimisation or application-specific use of grinding wheel bonds [2–4] and the influence of the process parameters on cutting edge quality [1, 5] and residual stress states [6]. The residual stress state is in this context important for the achievable tool life of the manufactured cutting tool [7] and subsequent coating processes [8] and therefore for the achievable tool quality. Despite the research efforts to enhance the productivity of tool grinding processes documented in literature, flute grinding is still the largest contributor to the process time and costs of discontinuous tool grinding processes.

The use of continuous generating grinding processes for the manufacturing of cutting tools is an example for the development of a new tool grinding process to meet the aforementioned challenges. The approach is based

on continuous generating grinding processes used in the production of conventional gears. The reason for this is that tool grinding processes and discontinuous production processes for gears are confronted with similar challenges, which can be overcome in gear manufacturing by using continuous generating grinding processes. For example, the use of continuous generating grinding processes allows high production rates to be achieved while maintaining a high surface quality of the gears through the application of wear compensation and shift strategies [9]. However, the application of continuous generating grinding processes for the manufacturing of cutting tools represents a comparatively novel approach which has not been extensively investigated or used in the industrial practice.

### 1.1 State of the art

Recent publications have already shown that it is generally possible to transfer continuous generating grinding processes from gear manufacturing to tool manufacturing [10, 11] and how an user-independent design of this process can be realised [11, 12]. The grinding worm geometry can be designed by applying an approach based on the Newton–Raphson method using the normalized tip clearance  $c_p^*$ , the normal module  $m_n$ , the normalized addendum modification  $x^*$  and the tooth root angle  $\alpha_{fp,l}$  of the grinding worm. Besides that, the target geometry has to be defined by its core diameter  $d_k$ , its outer diameter  $d$  as well as by its rake angle  $\gamma$  and its clearance angle  $\alpha$  to allow the design of the basic rack of the grinding worm [11, 12]. However, the wear of the grinding worms during the continuous generating grinding of cutting tools and inaccuracies during the dressing process of the grinding worm related to the wear of the dressing tool still present challenges for the productivity and precision of this process [11, 12]. Furthermore, the influence of the process parameters on the wear of the grinding worm and the process result have not been investigated in detail so far.

There is an extensive literature on continuous generating grinding of gears which focuses on investigating the process forces [13–16], their correlation with the process parameters [14, 16] as well as on the influence of the process parameters on the surface zone [16–18] and the grinding worm wear [16, 19, 20] since it is confronted with similar challenges as the ones mentioned above. Besides that there is a wide range of simulation based studies in the literature which aims on understanding the interrelationships in continuous generating grinding processes of gears and to improve these processes [17, 21–25]. But it is currently unknown whether this knowledge can be transferred to the continuous generating grinding of cutting tools. This paper therefore aims to investigate the

influence of the process parameters cutting speed, feed rate and depth of cut on the grinding result in continuous generating grinding of milling tools to contribute to an improved understanding of this process and to allow a knowledge-based consideration of the influence of these factors in future investigations.

## 2 Materials and methods

### 2.1 Workpiece material and milling tool geometry

In the investigations, steel 1.3343 (AISI M2, JIS SKH51, HSS) is used as workpiece material for all milling tools to be ground in this investigation. All milling tools have an intended outer diameter of 10 mm, a core diameter of 6.3 mm, six teeth, a helix angle of 33°, a rake angle of 1° and a clearance angle of 12°.

### 2.2 Experimental setup of the continuous generating process

All grinding experiments are conducted on a Walter Heli-tronic Vision 400 L tool grinding machine. All NC-Codes for the dressing and grinding operations are generated via the dexel-based simulation software IFW-CutS as described in [11, 12]. Vitrified bonded grinding wheels with CBN B76 as abrasive (Molemab GmbH) are used to perform the grinding operations. The dressing of the grinding worm profile is conducted with a CVD diamond form roll of the type NC40-C-150-R0.25-W40-12-TK (Dr. Kaiser Diamantwerkzeuge GmbH & Co. KG). The profile of the grinding worm is divided into lines with a step size of  $\Delta x_d = 60 \mu\text{m}$  (horizontal) and  $\Delta y_d = 8 \mu\text{m}$  (vertical) which are machined consecutively. The dressing process is performed with a cutting speed of the grinding tool of  $v_{cd} = 1.38 \text{ m/s}$ , a dressing speed ratio of  $q_d = 32.4$  and a feed velocity of the rotational axis of 95,000 °/min. The process parameters of the continuous generating grinding process are varied on three levels each as shown in Table 1. With regard to the variation of the radial depth of cut it must be considered that this means that the grinding process is performed in four strokes for a depth of cut of 0.4625 mm, in two strokes for a depth of cut of 0.925 mm and in one stroke for a depth of cut of 1.85 mm. The cooling lubricant used for

dressing and grinding is a grinding oil (Sintogrind MP830, Oelheld GmbH).

### 2.3 Measuring equipment

The geometry of the grinding worm is measured via a Leitz PMM 866 coordinate measuring machine after each dressing and grinding process. The macro geometry of the ground milling tools is measured via a Walter HeliCheck transmitted-light microscope. An Alicona Infinte Focus G5 focus variation microscope is used to investigate the cutting edge microgeometry of the milling tools after grinding. The roughness of the flank and rake face of the ground milling tools is measured optically via a Confovis Duo Vario confocal microscope and analysed with the software MountainsMap®.

## 3 Results and discussion

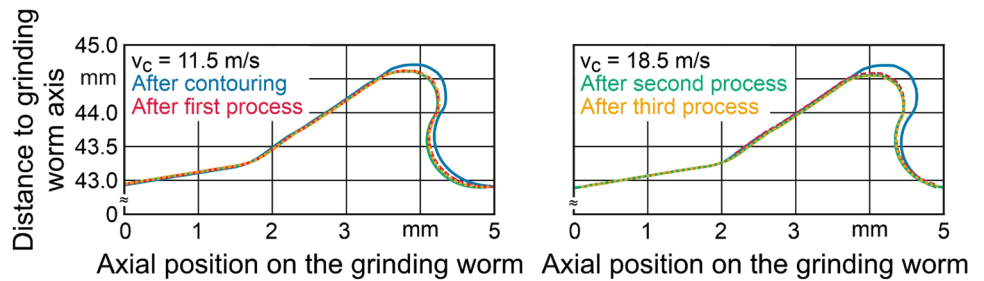
### 3.1 Influence of the cutting speed on the process result

For the investigation of the influence of the cutting speed, only  $v_c$  is varied in this step at the levels mentioned before. Feed and depth of cut are kept constant at  $f = 0.001 \text{ mm}$  and  $a_e = 0.46 \text{ mm}$ . To determine the influence of the cutting speed on the wear behaviour of the grinding worm, the grinding worm profiles are measured after one, two and three ground milling tools and compared with the grinding worm profile measured after dressing. The measured grinding worm profiles are shown in Fig. 1. Based on these measurements, three wear effects can be identified. Firstly, there are no macroscopic breakouts. It can be seen that the geometry of the grinding worm profile is reduced while the shape of the grinding worm profile is retained. Secondly, the wear of the grinding worm is especially pronounced during the grinding of the first milling tool. The wear of the grinding worm during the subsequent grinding operations is considerably lower in direct comparison. It is likely that the reason for this is an induction of microcracks into the vitrified bond by the dressing process. These microcracks grow during the first grinding process after dressing and contribute to the increased wear of the grinding worm in this step. Consequently, it must be assumed that the dressing process has a relevant influence on the wear behaviour of the grinding worm. However, the influence of the dressing process and its design on the wear behaviour has not been investigated in detail in this study. Thirdly, it can be seen that the grinding worm tooth tip is subject to a higher wear than the tooth root of the grinding worm. This is due to the kinematics of the process. The flute of the generated milling tool is ground by the

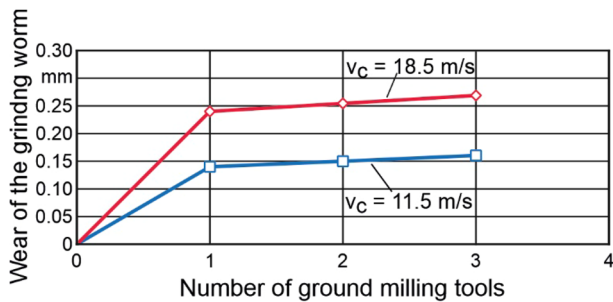
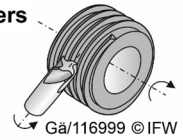
**Table 1** Parameter levels of the investigation

Parameter	Levels		
Cutting speed $v_c$ in m/s	11.5	15.0	18.5
Feed $f$ in mm	0.001	0.0025	0.005
Radial depth of cut $a_e$ in mm	0.4625	0.925	1.850

**Fig. 1** Grinding worm profiles dependent on the cutting speed



Toothing	Parameters of the grinding worm			Process parameters
$m_h = 1,64 \text{ mm}$	$k_{vP,l}^* = -1$	$k_{vP,r}^* = -0.3$	$h_a^* = -0.3$	$v_c = \text{var.}$
$z = 6$	$\alpha_{fP,l} = 80^\circ$	$\alpha_{fP,r} = 1^\circ$	$d_0 = 100 \text{ mm}$	$f = 0.001 \text{ mm}$
$\beta = 45^\circ$	$\alpha_{aP,l} = 54^\circ$	$\alpha_{aP,r} = 1^\circ$	$\rho_f = 0$	$a_e = 0.46 \text{ mm}$
$c_p^* = 0.27$	$sp_l = 0.2$	$sp_r = 0.1$	$\rho_a = 0$	$x^* = -1.1$



Toothing	Process parameters
$m_h = 1,64 \text{ mm}$	$v_c = \text{var.}$
$z = 6$	$f = 0.001 \text{ mm}$
$\beta = 45^\circ$	$a_e = 0.46 \text{ mm}$
$c_p^* = 0.27$	$x^* = -1.1$

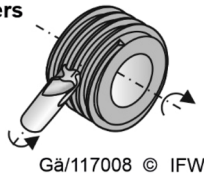


**Fig. 2** Influence of the cutting speed on the wear of the grinding worm

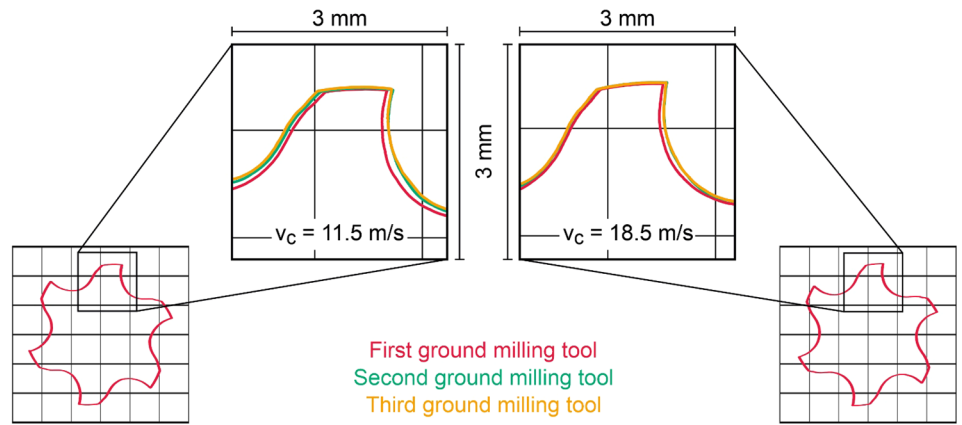
tip of the grinding worm tooth and the flank is ground by the tooth root of the grinding worm. Consequently, the material volume which is removed by the tooth tips of the grinding worm is much higher than the material volume removed by the tooth roots. This logically results in an increased load on the grinding worm tooth tip compared to the grinding worm tooth root.

In order to quantify the wear of the tooth tips and roots, the differences of the tooth tips and roots after dressing and each ground milling tool are measured in radial direction of the grinding worm. The wear is shown in Fig. 2 as a function of the number of ground milling tools. Regardless of the cutting speed, the linear flank area of the tooth root of the grinding worm, which generates the flank faces of the milling tool, does not show any measurable wear. After the first ground milling tool, the wear of the grinding worm tip at the cutting speed of  $v_c = 11.5 \text{ m/s}$  is 0.14 mm. The wear of the grinding worm tooth tip at

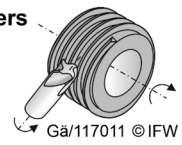
the cutting speed of  $v_c = 18.5 \text{ m/s}$  is 0.24 mm after the first ground milling tool. This is due to the higher load on the bond damaged by the dressing process. The next two grinding operations increase the wear of the tooth tips by 0.02 mm respectively by 0.03 mm at the cutting speed of  $v_c = 18.5 \text{ m/s}$ . It can be seen, that an increase in cutting speed mainly leads to an increase of the initial wear of the grinding worm at the tooth tips. In the investigated parameter range, the wear progress shows a comparable gradient despite the higher cutting speed. Consequently, apart from the initial wear, the cutting speed therefore does not have a major influence on the wear of the grinding worm.

In order to investigate the influence of the cutting speed related wear of the grinding worm on the geometrical accuracy of the ground milling tools, the three contours of the ground milling tools are compared. The contours are shown in Fig. 3. A positive effect on the use of the grinding worm is that the general shape of the remains the same, regardless of the grinding worm wear. The results indicate that neither the chosen cutting speed nor the observed wear of the grinding worm profile have an influence on the profile shape of the flank face. However, the width of the flank face increases with each ground milling tool, which further results in the increase of the outer diameter of the ground milling tools. At  $v_c = 11.5 \text{ m/s}$  the outer diameter of the first and third ground milling tool differ by 0.07 mm and by 0.09 mm at  $v_c = 18.5 \text{ m/s}$ . Since the increase of the cutting speed from  $v_c = 11.5 \text{ m/s}$  to  $v_c = 18.5 \text{ m/s}$  leads to an increase of the grinding worm tooth tip of 0.01 mm after the initial wear of the grinding worm due to the dressing a correlation between the outside diameter increase of the ground milling tool and the wear of the grinding worm tooth tip can be assumed. The wear behaviour of the tooth tips also affects the geometry of the flute of the ground milling tools. The increased wear of the tooth tips due to the increase in cutting speed leads to

**Fig. 3** Cutting speed-related influence of the grinding worm wear on the geometrical accuracy of the ground milling tools



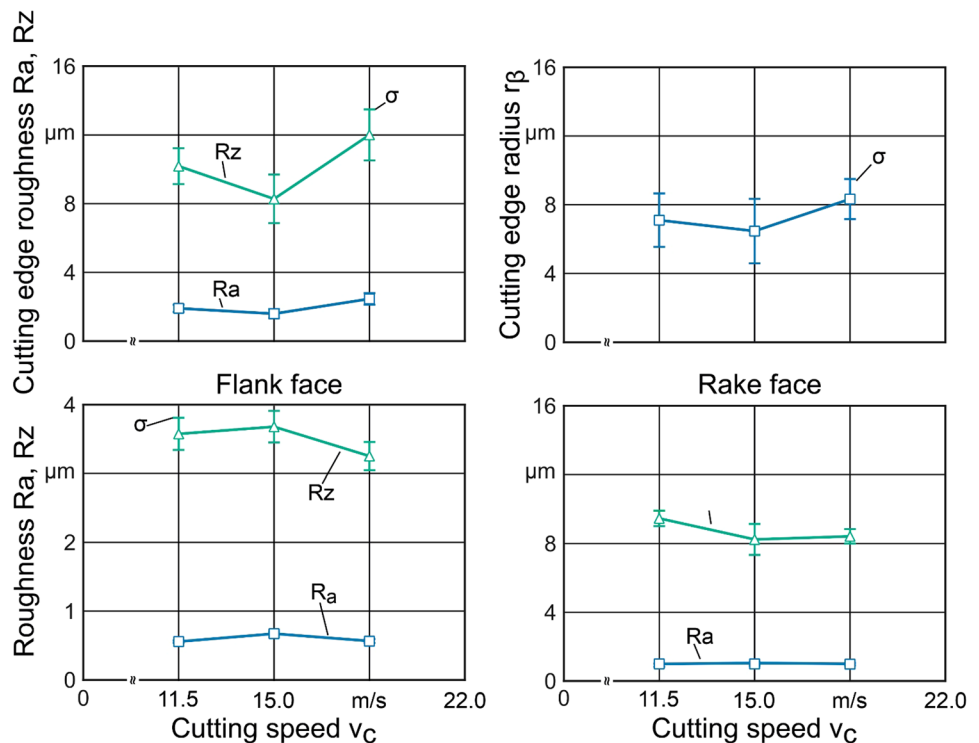
Toothing	Parameters of the grinding worm			Process parameters
$m_n = 1,64 \text{ mm}$	$k_{vP,l}^* = -1$	$k_{vP,r}^* = -0.3$	$h_a^* = -0.3$	$v_c = \text{var.}$
$z = 6$	$\alpha_{fP,l} = 80^\circ$	$\alpha_{fP,r} = 1^\circ$	$d_o = 100 \text{ mm}$	$f = 0.001 \text{ mm}$
$\beta = 45^\circ$	$\alpha_{aP,l} = 54^\circ$	$\alpha_{aP,r} = 1^\circ$	$\rho_f = 0$	$a_e = 0.46 \text{ mm}$
$c_p^* = 0.27$	$sp_{l}^* = 0.2$	$sp_{r}^* = 0.1$	$\rho_a = 0$	$x^* = -1.1$



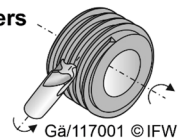
an increase in the core diameter of the ground milling tools. Due to the comparable contour of the ground milling tools, it can be assumed that the operational behaviour of the ground milling tools is not influenced by the

wear of the grinding worm. Furthermore, the change in core and outer diameter does not negatively affect the dimensional accuracy of the milling process, since the

**Fig. 4** Influence of the cutting speed on the cutting edge and roughness of the flank and rake face



Toothing	Parameters of the grinding worm			Process parameters
$m_n = 1,64 \text{ mm}$	$k_{vP,l}^* = -1$	$k_{vP,r}^* = -0.3$	$h_a^* = -0.3$	$v_c = \text{var.}$
$z = 6$	$\alpha_{fP,l} = 80^\circ$	$\alpha_{fP,r} = 1^\circ$	$d_o = 100 \text{ mm}$	$f = 0.001 \text{ mm}$
$\beta = 45^\circ$	$\alpha_{aP,l} = 54^\circ$	$\alpha_{aP,r} = 1^\circ$	$\rho_f = 0$	$a_e = 0.46 \text{ mm}$
$c_p^* = 0.27$	$sp_{l}^* = 0.2$	$sp_{r}^* = 0.1$	$\rho_a = 0$	$x^* = -1.1$



existing diameter of a milling tool is taken into account in every milling process.

Figure 4 shows the influence of the cutting speed on the cutting edge roughness and cutting edge radii on the one hand, and on the roughness of the flank and rake face of the ground milling tools on the other hand. The cutting edge roughness of the milling tools are in a range of  $R_a = 1.6\text{--}2.1\ \mu\text{m}$  and  $R_z = 8.3\text{--}10.4\ \mu\text{m}$ . As the cutting speed increases, the cutting edge roughness tends to increase. Due to the coupling of the rotational speed of the grinding tool and the workpiece, an increase of the cutting speed does not lead to any change in the single grain chip thickness. The cutting edge radii of the ground milling tools are in a range of  $r_\beta = 6.2\text{--}8.6\ \mu\text{m}$  and tend to increase as the cutting speed is increased. It can be assumed that this is due to the increasing wear and consequently the increasing geometric deviation of the grinding worm tooth tip as the cutting speed increases.

It can be seen that the roughness of the flank faces is lower than that of the rake faces. The roughness of are in a range of  $R_a = 0.6\text{--}0.7\ \mu\text{m}$  and  $R_z = 3.3\text{--}3.6\ \mu\text{m}$  on the flank face and  $R_a = 1.0\text{--}1.1\ \mu\text{m}$  and  $R_z = 8.2\text{--}9.5\ \mu\text{m}$  on the rake face. The reason for this is the smaller kinematic contact length between grinding worm and milling tool on the flank face than on the rake face which results from the kinematic of the grinding process. As a result, the coolant and chip transport on the rake face is worse than on the flank face. As a tendency, a higher cutting speed reduces the roughness of the rake and flank faces, although the influence in absolute values is only in a small range.

### 3.2 Influence of the feed on the process result

The measured grinding worm profiles after one, two and three ground milling tools are compared with the measured grinding worm profile after dressing in Fig. 5. As with the influence of the cutting speed, it can be seen that the grinding worm tooth tip is subject to higher wear than the

grinding worm tooth root. In contrast to  $v_c$  increasing the feed decreases the initial wear of the grinding worm tooth after the first grinding process. Furthermore, the wear of the grinding worm during the subsequent grinding operations is increased due to the increase of  $f$ .

The resulting wear curve is shown in Fig. 6. After grinding the first milling tool, the wear of the tooth tip is 0.14 mm for a feed of  $f = 0.001\ \text{mm}$ . The wear of the tooth tip at a feed of  $f = 0.005\ \text{mm}$  is 0.06 mm after grinding one milling tool. After the following two ground milling tools the wear of the tooth tip is increased by 0.02 mm for a feed of  $f = 0.001\ \text{mm}$ . Using a feed of  $f = 0.005\ \text{mm}$ , the wear of the grinding worm tooth tip shows a further increase of 0.09 mm after the second ground milling tool and an additional increase of 0.04 mm after the third grinding process. The increase of the feed leads to a reduction of the initial wear of the grinding worm tooth tip. It is most likely, that due to the increase of the single grain thickness and material removal rate caused by the increase of  $f$ , the

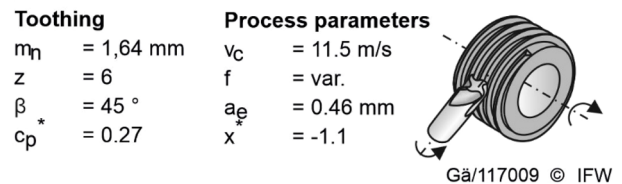
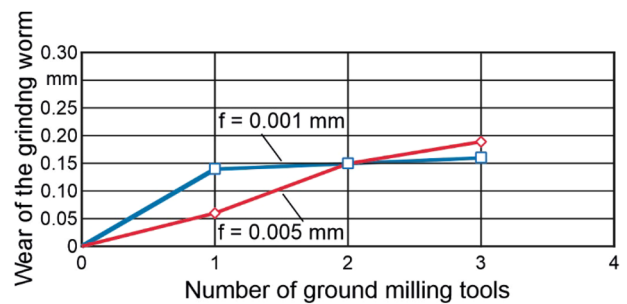
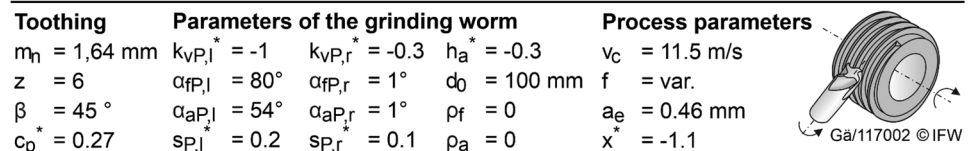
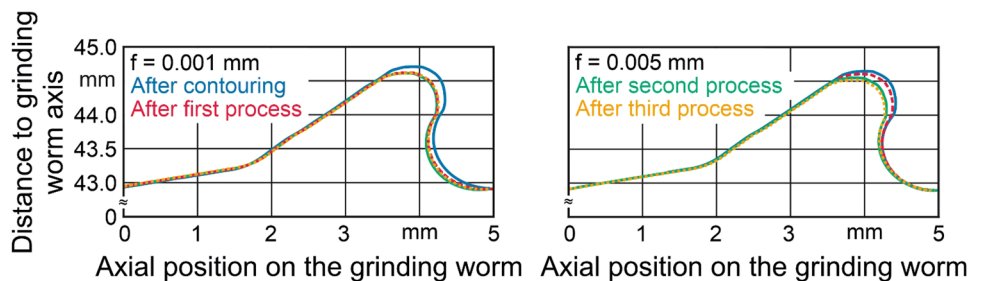


Fig. 6 Influence of the feed on the wear of the grinding worm

Fig. 5 Grinding worm profiles dependent on the feed



self-sharpening effect typical for vitrified bonds occurs earlier. At a low feed of  $f=0.001$  mm, the mechanical load is not sufficient to excite this effect. The consistent wear of the grinding worm tooth tip and the associated dimensional stability of the grinding worm tooth supports this hypothesis of self-sharpening. Consequently, a stable process can be realized by specifically adapting the process after the initial wear.

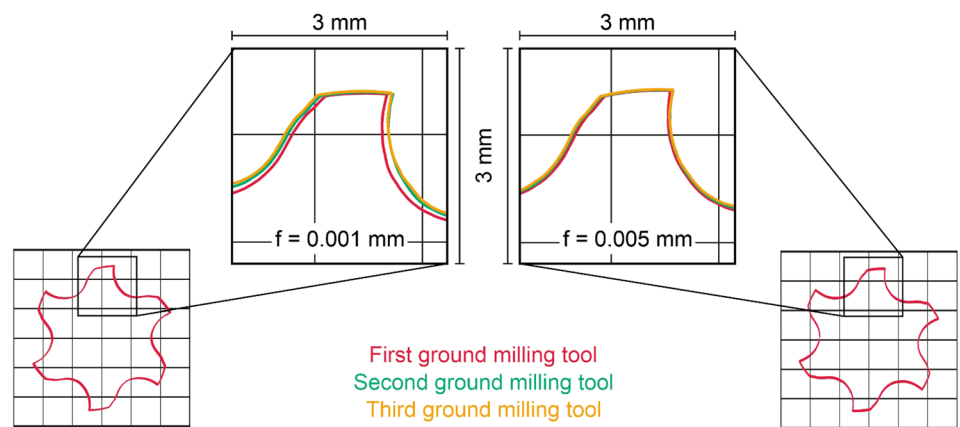
The feed-related influence of the grinding worm wear on the geometrical accuracy of the ground milling tools is shown in Fig. 7. The contours of the second and third milling tools ground by  $f=0.001$  mm show higher deviations from the contour of the first ground milling tool than those of the milling tools ground by  $f=0.005$  mm. At  $f=0.001$  mm the outer diameter of the first and the third milling tool differ by 0.1 mm and at  $f=0.005$  mm by 0.06 mm. Therefore, increasing  $f$  in the studied parameters leads to a decrease of the shape changes and thus the outer diameter changes of the ground milling tools, although the diameter of the grinding worm tooth decreases with every grinding process. With the increase of  $v_c$ , the outer diameter and core diameter of the ground milling tools show an increase after the first ground milling tool, although the diameter of the grinding worm tooth remains the same. These results supports the theory of the self-sharpening effect. Consequently, the cutting ability of the grinding worm is reduced, resulting in increased deflection of the milling tool from the grinding worm. Due to the self-sharpening effect in the processes with  $f=0.005$  mm, more sharp grains are exposed than with the process of  $f=0.001$  mm. This leads to a lower deflection of the milling tool during the grinding process. For the process this means that an increase of  $f$  leads to a stable

process and repeatable result, despite the linear wear of the grinding worm.

The influence of the feed on the cutting edge roughness, the cutting edge radii and the surface roughness are shown in Fig. 8. The cutting edge roughness increases due to the increase of the feed from  $R_a = 1.8 \mu\text{m}$  to  $R_a = 2.3 \mu\text{m}$  and from  $R_z = 9 \mu\text{m}$  to  $R_z = 11.5 \mu\text{m}$ . This increase of the cutting edge roughness results by the feed-related increase of the single grain chip thickness. As a result, each grain removes more material. In the area of the cutting edge, the emerge of the grains from the material consequently leads to an uneven cutting edge. An increase of the feed also leads to an increase of the cutting edge radii from  $r_\beta = 7.6 \mu\text{m}$  to  $r_\beta = 10.3 \mu\text{m}$ . This increase results from the geometrical change of the grinding worm tooth, which is caused by the wear of the grinding worm.

The roughness of the flank faces are in a range of  $R_a = 0.5\text{--}0.7 \mu\text{m}$  and  $R_z = 3.2\text{--}3.7 \mu\text{m}$ . In contrast to the influence of the cutting speed, an increase of the feed leads to an increase of the roughness on the flank faces and thus also to an increase of the cutting edge roughness. Since the flank faces are ground with the unworn tooth root of the grinding worm, it is likely that this effect results from the different engagement kinematics and thus the increase of the individual grain chip thickness due to the increase of the feed. Although the single grain chip thickness increases with the increase of  $f$ , the roughness of the rake face decreases from  $R_a = 1.1 \mu\text{m}$  to  $R_a = 0.9 \mu\text{m}$  and  $R_z = 9.2 \mu\text{m}$  to  $R_z = 8.7 \mu\text{m}$ . Despite the influence of the feed on the surface roughness of the ground milling tools, the measured values of the roughness are all at a comparable level. For this reason it can be assumed that the influence of the feed on the roughness has no significant effect

**Fig. 7** Feed-related influence of the grinding worm wear on the geometrical accuracy of the ground milling tools



Toothing	Parameters of the grinding worm			Process parameters
$m_n = 1,64$ mm	$k_{vP,l}^* = -1$	$k_{vP,r}^* = -0.3$	$h_a^* = -0.3$	$v_c = 11.5$ m/s
$z = 6$	$\alpha_{fP,l} = 80^\circ$	$\alpha_{fP,r} = 1^\circ$	$d_0 = 100$ mm	$f = \text{var.}$
$\beta = 45^\circ$	$\alpha_{aP,l} = 54^\circ$	$\alpha_{aP,r} = 1^\circ$	$\rho_f = 0$	$a_e = 0.46$ mm
$c_p^* = 0.27$	$s_{P,l} = 0.2$	$s_{P,r} = 0.1$	$\rho_a = 0$	$x^* = -1.1$

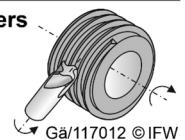
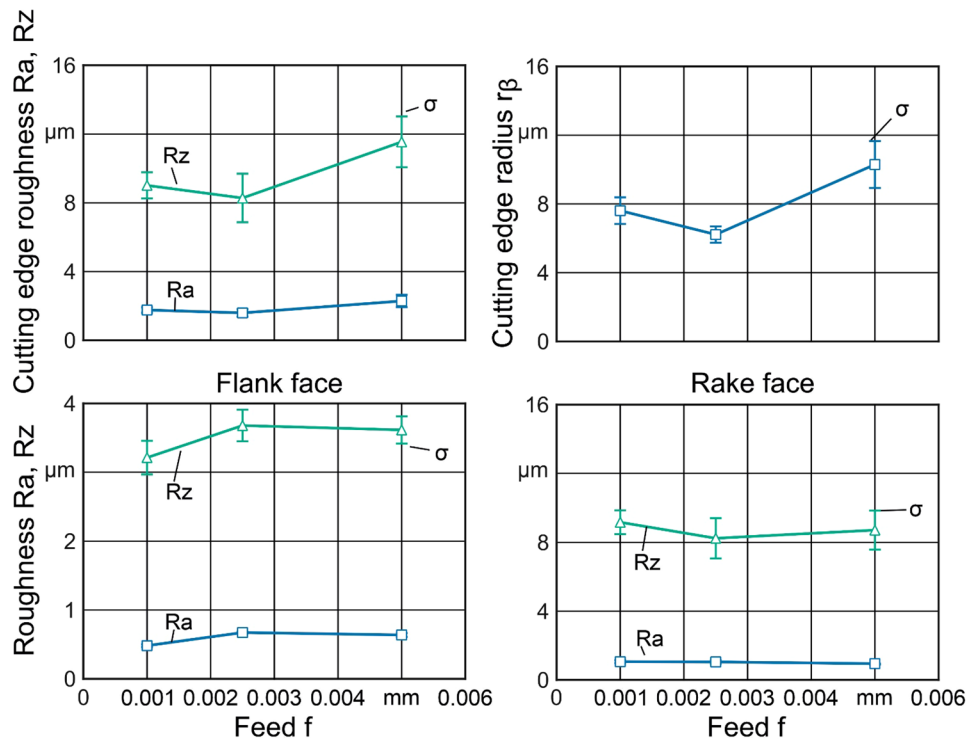
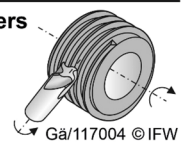


**Fig. 8** Influence of the feed on the cutting edge and roughness of the flank and rake face



Toothing	Parameters of the grinding worm			Process parameters
$m_n = 1,64 \text{ mm}$	$k_{vP,l}^* = -1$	$k_{vP,r}^* = -0.3$	$h_a^* = -0.3$	$v_c = 11.5 \text{ m/s}$
$z = 8$	$\alpha_{fP,l} = 80^\circ$	$\alpha_{fP,r} = 1^\circ$	$d_o = 100 \text{ mm}$	$f = \text{var.}$
$\beta = 45^\circ$	$\alpha_{aP,l} = 54^\circ$	$\alpha_{aP,r} = 1^\circ$	$\rho_f = 0$	$a_e = 0.46 \text{ mm}$
$c_p^* = 0.27$	$s_{P,l} = 0.2$	$s_{P,r} = 0.1$	$\rho_a = 0$	$x^* = -1.1$



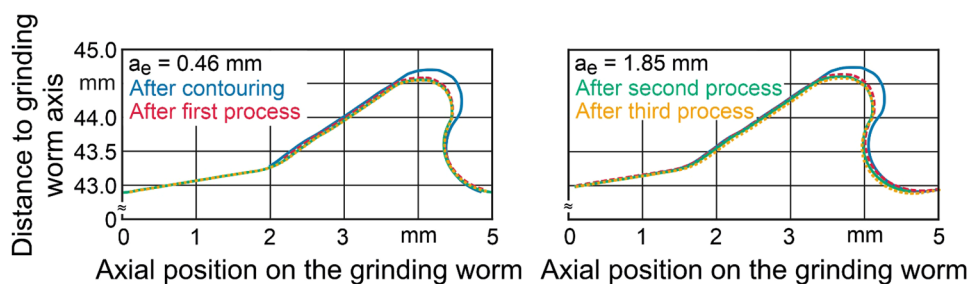
on the process behaviour of the milling tool. Therefore, the influence of the feed on the roughness of a milling tool can be considered negligible.

### 3.3 Influence of the radial depth of cut on the process result

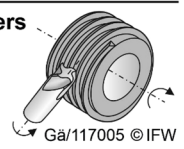
For the investigation of the radial depth of cut the cutting speed is held constant at  $v_c = 18.5 \text{ m/s}$  and the feed at

$f = 0.001 \text{ mm}$ . The radial depth of cut is varied according to Table 1. The grinding worm profiles dependent on the radial depth of cut are shown in Fig. 9. Independent of the radial depth of cut, the wear of the grinding worm is especially pronounced during the grinding of the first milling tool. The wear of the grinding worm during the subsequent grinding operations is considerably lower in direct comparison. Furthermore, the wear of the tooth tips

**Fig. 9** Grinding worm profiles dependent on the radial depth of cut



Toothing	Parameters of the grinding worm			Process parameters
$m_n = 1,64 \text{ mm}$	$k_{vP,l}^* = -1$	$k_{vP,r}^* = -0.3$	$h_a^* = -0.3$	$v_c = 18.5 \text{ m/s}$
$z = 6$	$\alpha_{fP,l} = 80^\circ$	$\alpha_{fP,r} = 1^\circ$	$d_o = 100 \text{ mm}$	$f = 0.001 \text{ mm}$
$\beta = 45^\circ$	$\alpha_{aP,l} = 54^\circ$	$\alpha_{aP,r} = 1^\circ$	$\rho_f = 0$	$a_e = \text{var.}$
$c_p^* = 0.27$	$s_{P,l} = 0.2$	$s_{P,r} = 0.1$	$\rho_a = 0$	$x^* = -1.1$





after the first ground milling tool is at a comparable level regardless of the depth of cut.

The wear curve of the investigation of the radial depth of cut is shown in Fig. 10. The tooth tips show a wear of 0.24 mm for a radial depth of cut of  $a_e = 0.46$  mm after grinding one milling tool. The following two grinding processes lead to a further wear of 0.03 mm in this case. An increase of the radial depth of a cut to  $a_e = 1.85$  mm leads to wear of the grinding worm tooth tip of 0.26 mm after the first ground milling tool. The following two grinding processes lead to a further wear of 0.02 mm. Despite the different depth of cut, the wear curves show the same degressive course, although the material removal rate

differs by the factor of four. Consequently, in the investigated range increasing the radial depth of cut offers the potential to increase the productivity of the process without affecting the wear behavior of the grinding worm. The increase of the radial depth of cut from  $a_e = 0.46$  mm to  $a_e = 1.85$  mm results in a wear of the grinding worm tooth root. This wear at the tooth root results from the distribution of the load on the whole tooth instead.

The radial depth of cut-related influence of the grinding worm wear on the geometrical accuracy of the ground milling tools is shown in Fig. 11. In general, the differences of the ground milling tool contours are on a comparable level independent of the used radial depth of cut. As the radial depth of cut does not have huge influence on the wear behaviour of the grinding worm tooth tip, an increase of the depth of cut does not affect the geometric accuracy of the flute and the width of the flank face of the ground milling tools. Furthermore, the occurring wear of the tooth root at  $a_e = 1.85$  mm does not influence the outer diameter and the geometry of the flank faces.

Despite the increase in productivity by the factor of four, the increase of the radial depth of cut results neither in an increased wear of the grinding worm nor in increased geometric deviations of the ground milling tool from the intended geometry. The influence of the radial depth of cut on the cutting edge roughness and radius is shown in Fig. 12. The cutting edge roughness tends to increase for a higher radial depth of cut, which is caused by the greater single grain chip thickness. An increase of the radial depth of a cut from  $a_e = 0.46$  mm to  $a_e = 1.85$  mm causes an increase of the cutting edge radii of the generated milling tools. The reason is that due to the increase of the radial depth of cut the increased material removal rate favours

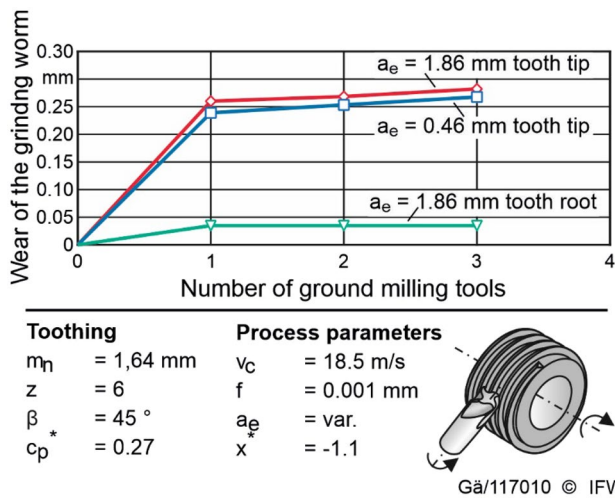
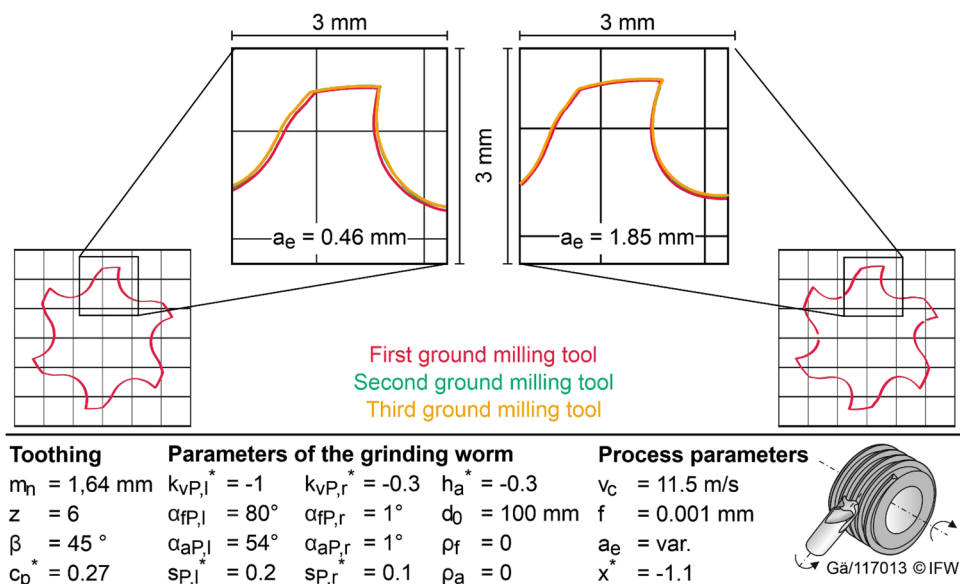
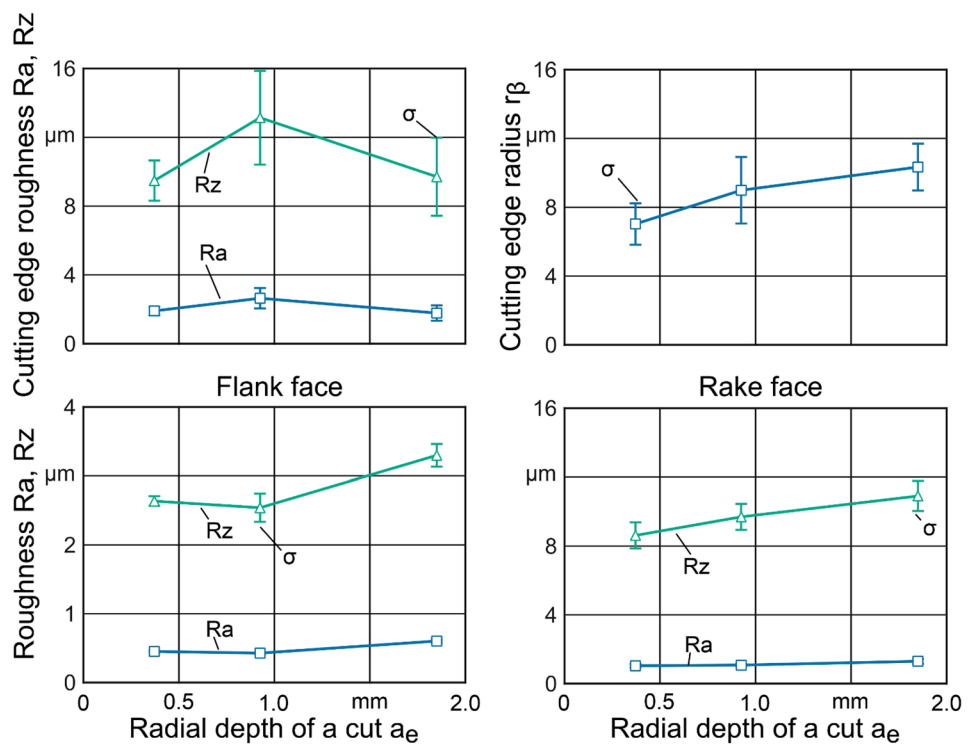



Fig. 10 Influence of the radial depth of cut on the wear of the grinding worm

Fig. 11 Radial depth-related influence of the grinding worm wear on the geometrical accuracy of the ground milling tools



**Fig. 12** Influence of the radial depth of cut on the cutting edge and roughness of the flank and rake face



Toothing		Parameters of the grinding worm			Process parameters	
$m_n = 1,64$ mm	$k_{VP,l}^* = -1$	$k_{VP,r}^* = -0.3$	$h_a^* = -0.3$	$v_c = 18.5$ m/s		
$z = 6$	$\alpha_{fP,l} = 80^\circ$	$\alpha_{fP,r} = 1^\circ$	$d_0 = 100$ mm	$f = 0.001$ mm		
$\beta = 45^\circ$	$\alpha_{aP,l} = 54^\circ$	$\alpha_{aP,r} = 1^\circ$	$\rho_f = 0$	$a_e = \text{var.}$		
$c_p^* = 0.27$	$s_{P,l} = 0.2$	$s_{P,r} = 0.1$	$\rho_a = 0$	$x^* = -1.1$		

plastic deformation of the workpiece material at the cutting edge. Consequently, the sharp edges of the generated cutting tool are rounded.

Figure 12 also displays, that an increase of the radial depth of cut leads to a linear increase of the roughness of the rake and flank faces. This increase in roughness results from the deeper penetration of the grains into the workpiece, which is caused by the higher infeed depth.

### 4 Conclusions

The adaption of the continuous generating grinding processes to tool grinding processes has the potential to increase the productivity of the manufacturing of cutting tools and to generate economic benefits. Due to the innovative nature of the process, the utilization of continuous generating grinding processes for tool grinding has not yet been thoroughly investigated. Thus, the objective of this study is to examine the initial indications of the impact of cutting speed, feed and radial depth of cut on the continuous generating grinding process, in order to generate preliminary insights for process design.

In this study it was demonstrated that the wear behaviour of the grinding worms with a vitrified bond and CBN proceeds without breakouts. This indicates that no sudden bond failure occurs due to excessive process loads. The wear of the grinding worm primarily takes place on the tips of the grinding worm teeth. This wear of the grinding worm tooth tip leads deviations of the milling tool and to an increase of both the core and outer diameter. Nevertheless, it can be assumed that the resulting deviations do not have significant influence on the performance of the milling tools. Increased initial wear of the grinding worm occurs during the first grinding process. Investigations by Fujimoto et al. [26] reflect comparable results when dressing vitrified bonded CBN grinding wheels. Here, the increased initial wear and characteristic drop in grinding forces were associated with the loss of unstable grains at edges and the formation of new sharp cutting edges [26, 27]. Based on the investigations, it can be assumed that a self-sharpening effect typical for vitrified bonds [26] occurs with increasing mechanical load and that the wear behaviour of the grinding worm is influenced by this. Increasing the cutting speed leads to an increase of the initial wear of the grinding worm tooth after the

dressing process. The wear of the grinding worm after the initial wear is not influenced by the cutting speed. Furthermore, the influence of the cutting speed on the cutting edge quality and roughness of the flank and rake face of the ground milling cutters is low. Consequently, it can be assumed that the cutting speed after the initial wear has no influence on the microwear of the grinding worm. An increase of the feed leads to a reduction of the initial wear of the grinding worm tooth, but to a further increase of the wear of the grinding worm tooth after the initial wear. The cutting edge roughness of the generated milling tool is mainly influenced by the feed. An increase of the feed leads to an increase of the cutting edge roughness, but also of the cutting edge radius. An increase of the feed also leads to an increase of the roughness of the flank face, although the influence is negligible due to the small change. This leads to the presumed conclusion, that the feed does influence the wear of the microwear of the grinding worm after the initial wear. On the one hand increasing the depth of cut by a factor of four has shown that the wear of the grinding worm tip is not affected. On the other hand the increase in the depth of cut also extends the wear to the tooth root of the grinding worm, which does not lead to any significant deviation of the cutter geometry. An increase in the depth of cut leads to an increase in both the cutting edge radius and the surface properties of the flank and rake of the ground cutters. Based on the results of this investigation, the following conclusions can be drawn:

- Vitri-fied bonded CBN grinding wheels are suitable for dressing into grinding worms.
- The continuous generating grinding process is capable of producing cutting tools with the aid of grinding worms.
- For increasing the productivity of the process  $a_e$  should be selected to a maximum,  $v_c$  should be increased as much as the wear of the grinding worm allows and  $f$  should be low.
- The investigation of the dressing offers further potential to improve the productivity of the continuous generating grinding process.

**Acknowledgements** The authors would like to thank the German Research Foundation (DFG) for supporting the project DE 447/153-2 "Continuous Generating Grinding of Cutting Tools 2".

**Author contributions** BD was responsible for funding acquisition and project supervision. He also reviewed and edited the manuscript in the writing process together with BB. PW was responsible for project administration. NG conducted the experiments. He analysed the data and wrote the manuscript together with PW, BB and BD.

**Funding** Open Access funding enabled and organized by Projekt DEAL. This work was supported by the German Research Foundation (DFG) under Grant Number DE 447/153-2.

**Data availability** Not applicable.

**Code availability** Not applicable.

## Declarations

**Conflict of interest** This work was supported by the German Research Foundation (DFG) under Grant Number DE 447/153-2. The funders had no role in the design of this work, in the collection, analyses, and interpretation of the data, in the writing of the manuscript, or in the decision to publish the results. On behalf of all authors, the corresponding author states that the authors have no competing interests to declare that are relevant to the content of this article.

**Open Access** This article is licensed under a Creative Commons Attribution 4.0 International License, which permits use, sharing, adaptation, distribution and reproduction in any medium or format, as long as you give appropriate credit to the original author(s) and the source, provide a link to the Creative Commons licence, and indicate if changes were made. The images or other third party material in this article are included in the article's Creative Commons licence, unless indicated otherwise in a credit line to the material. If material is not included in the article's Creative Commons licence and your intended use is not permitted by statutory regulation or exceeds the permitted use, you will need to obtain permission directly from the copyright holder. To view a copy of this licence, visit <http://creativecommons.org/licenses/by/4.0/>.

## References

1. Uhlmann E, Hübert C (2011) Tool grinding of end mill cutting tools made from high performance ceramics and cemented carbides. *CIRP Ann Manuf Technol* 60:359–362. <https://doi.org/10.1016/j.cirp.2011.03.106>
2. Rabiey M, Jochum N, Kuster F (2013) High performance grinding of zirconium oxide (ZrO<sub>2</sub>) using hybrid bond diamond tools. *CIRP Ann Manuf Technol* 62(1):343–346. <https://doi.org/10.1016/j.cirp.2013.03.073>
3. Uhlmann E, Schröder N (2015) Advances in tool grinding and development of end mills for machining of fiber reinforced plastics. *Procedia CIRP* 35:38–44. <https://doi.org/10.1016/j.procir.2015.08.053>
4. Wang S-X, Geng L, Liu X-J, Geng B, Niu S-C (2009) Manufacture of a new kind diamond grinding wheel with Al-base bonding agent. *J Mater Process Technol* 209:1871–1876. <https://doi.org/10.1016/j.jmatprotec.2008.04.045>
5. Ohmori H, Katahira K, Naruse T, Uehara Y, Nakao A, Mizutani M (2007) Microscopic grinding effects in fabrication of ultra-fine micro tools. *CIRP Ann* 56(1):569–572. <https://doi.org/10.1016/j.cirp.2007.05.136>
6. Zhao X, Zhang S, Zhen W (2016) Potential failure cause analysis of tungsten carbide end mills for titanium alloy machining. *Eng Fail Anal* 66:321–327. <https://doi.org/10.1016/j.engfailanal.2016.05.004>
7. Teppernegg T, Klünsner T, Angerer P, Tritremmel C, Czettl C, Keckes J, Ebner R, Pippan R (2014) Evolution of residual stress and damage in coated hard metal milling inserts over the

- complete tool life. *Int J Refract Metal Hard Mater* 47:80–85. <https://doi.org/10.1016/j.ijrmhm.2014.07.005>
8. Uhlmann E, Klein K (2001) Method for the analysis of residual stress induced failure in thin films. *Ann CIRP* 50(1):401–404. [https://doi.org/10.1016/S0007-8506\(07\)62150-7](https://doi.org/10.1016/S0007-8506(07)62150-7)
  9. Karpuschewski B, Knoche H-J, Hipke M (2008) Gear finishing by abrasive processes. *CIRP Ann* 57(2):621–640. <https://doi.org/10.1016/j.cirp.2008.09.002>
  10. Denkena B, Krödel A, Theuer M (2020) Novel continuous generating grinding process for the production of cutting tools. *CIRP J Manuf Sci Technol* 28:1–7
  11. Theuer M (2020) Kontinuierliches Wälzschleifen von Zerspanwerkzeugen. Leibniz University Hannover, Hannover
  12. Denkena B, Bergmann B, Theuer M, Wolters P (2022) Geometrical process design during continuous generating grinding of cutting tools. *Int J Adv Manuf Technol* 121:3871–3882. <https://doi.org/10.1007/s00170-022-09573-7>
  13. Kruszyński BW, Midera S, Kaczmarek J (1998) Forces in generating gear grinding – theoretical and experimental Approach. *CIRP Ann* 47(1):287–290. [https://doi.org/10.1016/S0007-8506\(07\)62835-2](https://doi.org/10.1016/S0007-8506(07)62835-2)
  14. Brecher C, Brumm M, Hübner F (2015) Approach for the calculation of cutting forces in generating gear grinding. *Procedia CIRP* 33:287–292. <https://doi.org/10.1016/j.procir.2015.06.051>
  15. de Oliveira Löhner P, Solf M, Brimmers J, Bergs T (2022) Force modeling in generating gear grinding considering the grinding worm topography. *Procedia CIRP* 115:66–71. <https://doi.org/10.1016/j.procir.2022.10.051>
  16. Köhler J, Schindler A, Woiwode S (2012) Continuous generating grinding—tooth root machining and use of CBN-tools. *CIRP Ann* 61(1):291–294. <https://doi.org/10.1016/j.cirp.2012.03.033>
  17. Klocke F, Brumm M, Reimann J (2013) Modeling of surface zone influences in generating gear grinding. *Procedia CIRP* 8:21–26. <https://doi.org/10.1016/j.procir.2013.06.059>
  18. Schrank M, Brimmers J, Bergs T (2021) Potentials of vitrified and elastic bond fine grinding worms in continuous generating gear grinding. *J Manuf Mater Process* 5(1):4. <https://doi.org/10.3390/jmmp5010004>
  19. Tao Y, Li G, Cao B, Jiang L (2022) Grinding worm wear evaluation and its influence on gear surface topography in continuous generating gear grinding. *Int J Adv Manuf Technol* 123:3301–3311. <https://doi.org/10.1007/s00170-022-10368-z>
  20. Ophrey M, Löpenhaus C, Klocke F (2015) Influence of tool specification and machining parameters on the wear behaviour at generating gear grinding. *Appl Mech Mater* 794:231–238. <https://doi.org/10.4028/www.scientific.net/amm.794.231>
  21. Dietz C, Wegener K, Thyssen W (2016) Continuous generating grinding: machine tool optimisation by coupled manufacturing simulation. *J Manuf Process* 23:211–221. <https://doi.org/10.1016/j.jmapro.2016.06.024>
  22. Haifeng C, Tang J, Zhou W (2013) Modeling and predicting of surface roughness for generating grinding gear. *J Mater Process Technol* 213(5):717–721. <https://doi.org/10.1016/j.jmatprotec.2012.11.017>
  23. Guo H, Wang X, Zhao N, Fu B, Liu L (2022) Simulation analysis and experiment of instantaneous temperature field for grinding face gear with a grinding worm. *Int J Adv Manuf Technol* 120:4989–5001. <https://doi.org/10.1007/s00170-022-09036-z>
  24. Böttger J, Kimme S, Drossel W-G (2019) Simulation of dressing process for continuous generating gear grinding. *Procedia CIRP* 79:280–285. <https://doi.org/10.1016/j.procir.2019.02.067>
  25. Denkena B, Köhler J, Schindler A, Woiwode S (2014) Continuous generating grinding—material engagement in gear tooth root machining. *Mech Mach Theory* 81:11–20. <https://doi.org/10.1016/j.mechmachtheory.2014.06.008>
  26. Fujimoto M, Ichida Y, Sato R, Morimoto Y (2006) Characterization of wheel surface topography in cBN grinding. *JSME Int J Ser C* 19(1):106–113. <https://doi.org/10.1299/jsmec.49.106>
  27. Jackson MJ, Hitchiner MP (2011) Abrasive tools and bonding systems. In: Jackson M, Davim JP (eds) *Machining with abrasives*, 1st edn. Springer, New York, pp 1–77

**Publisher's Note** Springer Nature remains neutral with regard to jurisdictional claims in published maps and institutional affiliations.